Inhomogeneous space-time structure and two-pion interferometry in NEXSPHERIO model*

REN Yan-Yu(任延宇)[1] Efaaf M. J.[2] ZHANG Wei-Ning(张卫宁)[1,2,3;1)]

[1] Department of Physics, Harbin Institute of Technology, Harbin 150006, China
[2] School of Physics and Optoelectronic Technology, Dalian University of Technology, Dalian 116024, China
[3] Center of Theoretical Nuclear Physics, National Laboratory of Heavy Ion Accelerator of Lanzhou, Lanzhou 730000, China

Abstract We examine the space-time structure of particle-emitting source and two-pion interferometry in a smoothed hydrodynamic model with fluctuating initial conditions. An equation of state with a crossover transition between quark-gluon plasma and hadronic gas is adopted in the description of the system evolution. We find that the fluctuating initial conditions lead to inhomogeneous particle-emitting sources. The interferometry results of $R_{\rm s}$ and $R_{\rm o}$ indicate that both the source size and the duration of pion emission decrease when the freeze-out temperature increases. The values of $R_{\rm o}/R_{\rm s}$ obtained by our simulated two-pion interferometry are consistent with the previous results of smoothed particle hydrodynamics, and smaller than those calculated in usual hydrodynamic models.

Key words two-pion interferometry, space-time structure, NEXSPHERIO model, inhomogeneous sources

PACS 25.75.-q, 25.75.Gz

1 Introduction

Hydrodynamics has been extensively used in high energy heavy ion collisions to describe the system evolution [1–4]. After assuming an equation of state (EOS), the hydrodynamic approach can provide a direct link between the early states of the hot and dense matter and final observable quantities in the collisions. In usual hydrodynamic models, the initial conditions are treated as smoothed distributions. However, the initial matter distribution on event-by-event basis is far from being smoothed and with large fluctuation. This large fluctuation may lead to an inhomogeneous particle-emitting source and finally affect the source space-time observables [5–9]. It is interesting to investigate the space-time structure of the system with this initial fluctuation and its effect on the space-time observables.

Two-pion Hanbury-Brown-Twiss (HBT) interferometry is a valid tool for probing the space-time structure of particle-emitting sources [10–13]. In Ref. [6] a two-pion HBT analysis is applied to the hydrodynamic evolution sources at RHIC energy and with the fluctuating initial conditions. The authors use a smoothed particle hydrodynamic code, NEXSPHERIO [14–16], to describe the source evolution and calculate the HBT correlation functions with the distribution function $f(x,k)$ of the source [6]. The EOS they used has a first-order phase transition between the quark-gluon plasma (QGP) and hadronic gas. In this paper, we will use NEXSPHERIO with a more realistic EOS of crossover transition to describe the source evolution. We will examine the inhomogeneous space-time structure of the sources directly and apply a simulated two-pion HBT analysis [17, 18] to the sources. All of our analyses are aimed at gold-gold collision at $\sqrt{s_{\rm NN}}=200$ GeV.

The paper is organized as follows. In Sec. 2, we introduce the NEXSPHERIO briefly and examine the inhomogeneous space-time structure of the system. In Sec. 3, we investigate the two-pion HBT correlations in NEXSPHERIO model with different impact parameters and freeze-out temperatures. We extract the HBT radii for the sources with different condi-

Received 9 June 2009

* Supported by National Natural Science Foundation of China (10775024) and Foundation of Theoretical Nuclear Physics Center of National Laboratory of Heavy Ion Accelerator of Lanzhou

1) E-mail: weiningzh@hotmail.com

tions and compare them with that in usual hydrodynamical models and experimental data. Finally, the conclusions are given in Sec. 4.

2 Space-time structure of the system in NEXSPHERIO model

NEXSPHERIO is a combination of NEXUS and SPHERIO codes, where NEXUS gives the initial conditions of the collisions on event-by-event basis [19] and SPHERIO describes the system evolution with smoothed particle hydrodynamics [14–16]. The initial quantities provided by NEXUS are event-by-event fluctuated. Smoothed particle hydrodynamics is suitable for realing the system evolution with large fluctuating initial conditions [14–16]. It has been used in high energy heavy ion collisions for a wide range of problems [6, 8, 14–16, 20–22].

We first consider two kinds of EOS. The first one, EOS-Ⅰ, has a first-order phase transition at $T_c = 160$ MeV between the QGP and hadronic resonance gas as used in the NEXSPHERIO version in Refs. [6, 14–16]. The second one, EOS-Ⅱ, is obtained by smoothing the EOS-Ⅰ in the transition region with the entropy density suggested by QCD lattice results [17, 23–25]. Fig. 1 shows the relations of the thermodynamical quantities for the systems evolving with the EOS-Ⅰ (grey) and EOS-Ⅱ (black), where s, ϵ, P are entropy density, energy density, and pressure of the system. The width of the transition ΔT for the EOS-Ⅱ is taken to be $0.1T_c$ [25].

In Fig. 2 we show the evolution of NEXSPHERIO events for $\sqrt{s_{NN}} = 200$ GeV Au+Au collisions with the EOS-Ⅰ and EOS-Ⅱ. Figs. 2(a), (b), (c) and (d) are the pictures of the transverse distributions of energy density for one NEXSPHERIO event in the collision with impact parameter $b = 0$ fm and evolving with EOS-Ⅰ. The pictures are taken for the region ($|x, y| < 12$ fm and $|z| < 0.83$ fm) and at $t = 1, 4, 7$, and 10 fm/c with an exposure of $\Delta t = 0.3$ fm/c. Figs. 2(a′), (b′), (c′) and (d′) are the pictures for the event with the same initial conditions but evolving with EOS-Ⅱ. One can see that the systems are inhomogeneous in space and time. There are many "lumps" in the systems both for the events evolving with the EOS-Ⅰ and the EOS-Ⅱ. Because the transition between the QGP and hadronic gas is likely of crossover type in the heavy ion collisions at RHIC energy [26, 27], we will use only the EOS-Ⅱ in our calculations later.

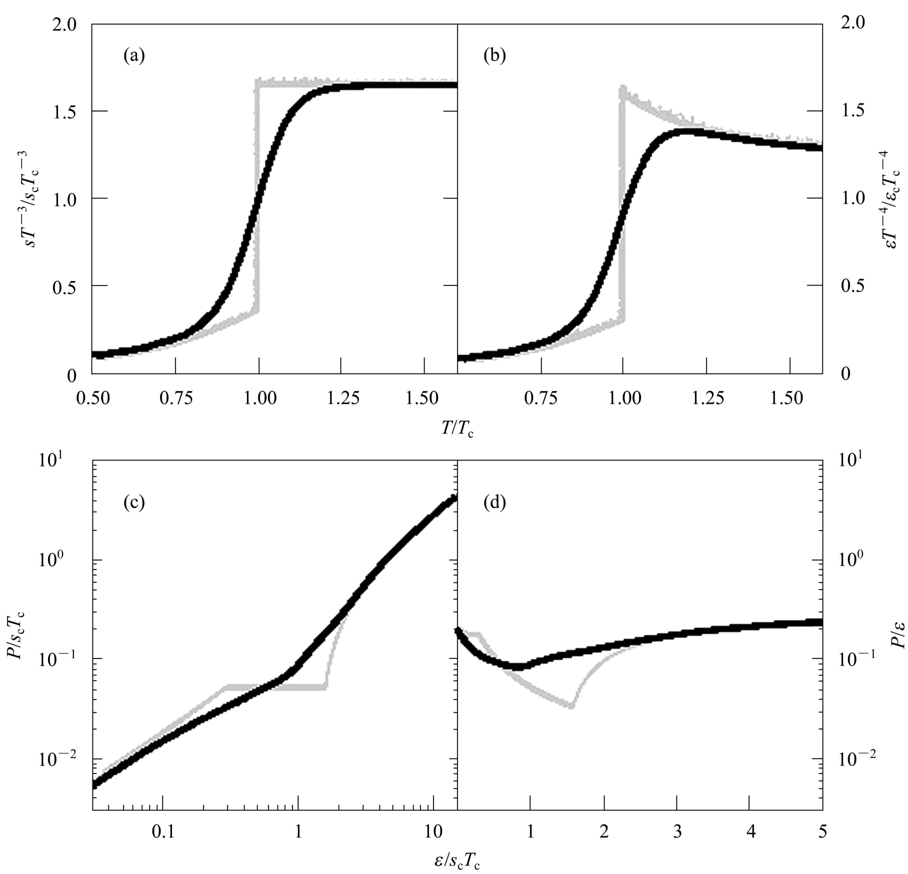

Fig. 1. (a) entropy density s, (b) energy density ϵ, (c) pressure P, and (d) P/ϵ of the systems evolving with EOS-Ⅰ (grey) and EOS-Ⅱ (black).

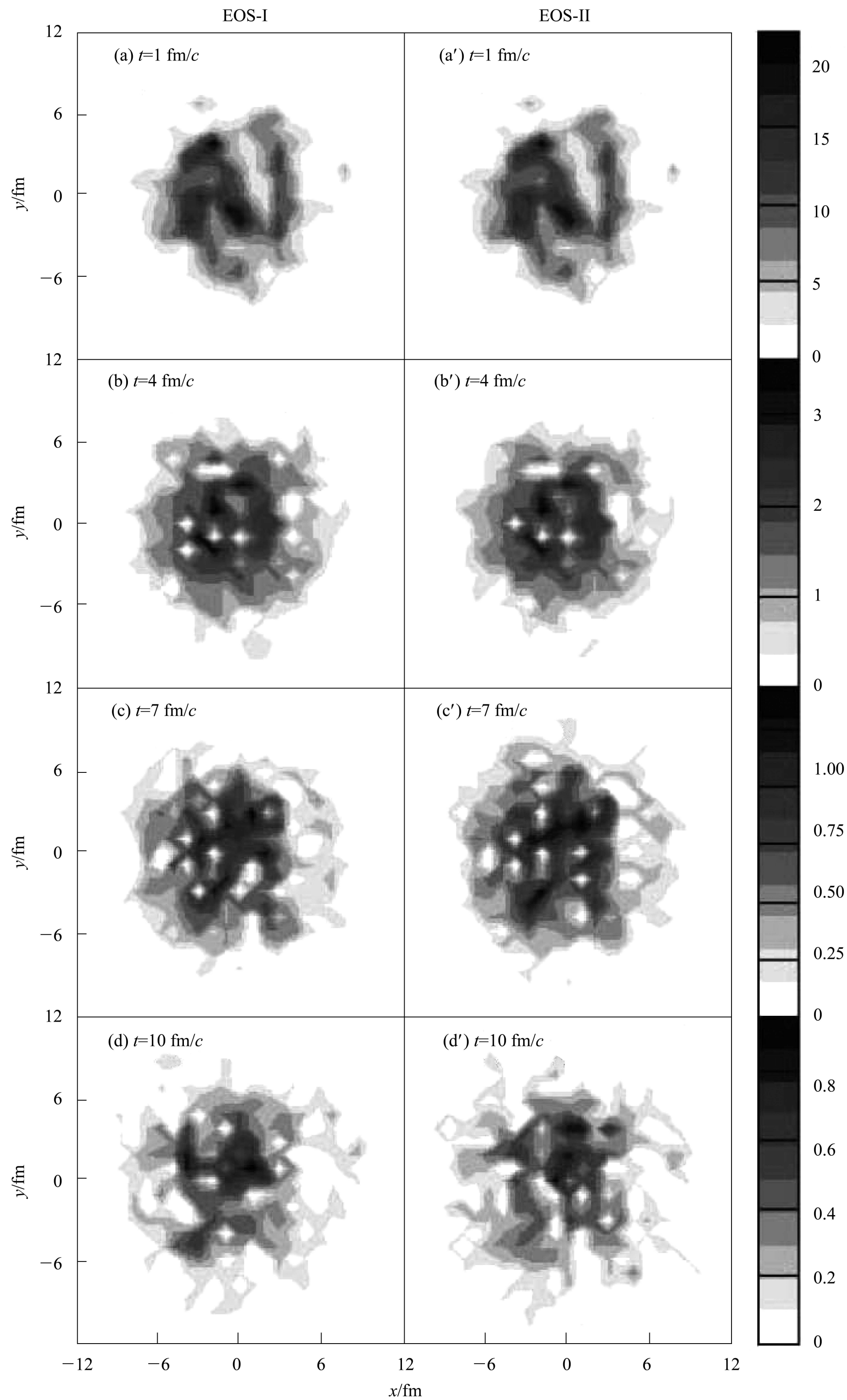

Fig. 2. Transverse distributions of energy density of the events evolving with EOS-Ⅰ ((a)–(d)) and EOS-Ⅱ ((a′)–(d′)) at different times for $\sqrt{s_{\rm NN}}=200$ GeV Au+Au collisions, $b=0$ fm. The unit of energy density is $\rm GeV/fm^3$.

Figure 3 shows the pictures of the transverse distributions of energy density for events with different impact parameters. One can see that both the system size and the number of lumps in the system decrease with the impact parameter increasing.

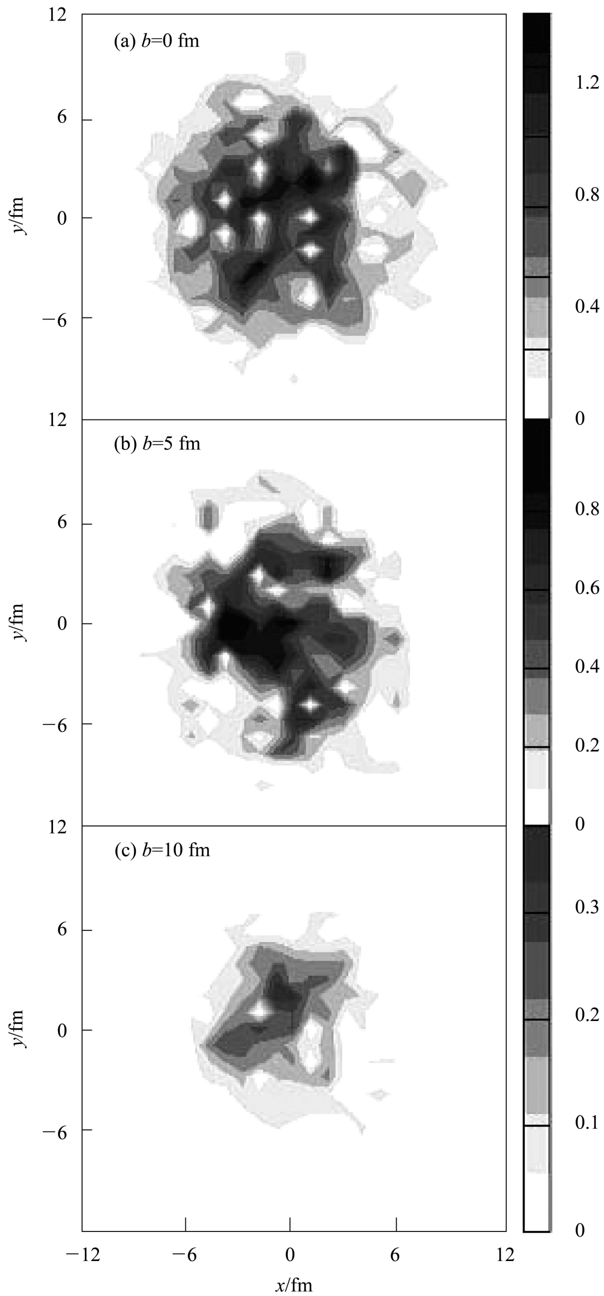

Fig. 3. Transverse distributions of energy density of the systems with different impact parameters at $t = 7$ fm/c. The unit of energy density is GeV/fm^3.

3 Two-pion HBT analysis

Assuming that the final identical pions are emitted at the space-time configuration characterized by a freeze-out temperature $T_{\rm f}$, we can generate the pion momenta $p_i (i = 1, 2)$ according to Bose-Einstein distribution and construct the two-pion correlation function $C(q_{\rm o}, q_{\rm s}, q_{\rm l})$ in model calculations [7, 18]. Here $q_{\rm o}$, $q_{\rm s}$, and $q_{\rm l}$ are the components of "out", "side", and "long" of relative momentum of pion pair [28, 29]. The HBT radii are extracted by fitting the correlation function with the following parametrized correlation function:

$$C(q_{\rm o}, q_{\rm s}, q_{\rm l}) = 1 + \lambda \exp(-q_{\rm o}^2 R_{\rm o}^2 - q_{\rm s}^2 R_{\rm s}^2 - q_{\rm l}^2 R_{\rm l}^2) . \quad (1)$$

In Fig. 4 we show the two-pion correlation functions $C(q_{\rm o}, q_{\rm s}, q_{\rm l})$ for different impact parameters in our calculations with NEXSPHERIO. The freeze-out temperature is taken to be 150 MeV. For each impact parameter, we generate 40 single events, each of them provides $N_{\pi\pi} = 10^6$ correlated pion pairs in the relative momentum region ($q_{\rm o}, q_{\rm s}, q_{\rm l} \leqslant 200$ MeV/c). The numbers of the pion pairs in the relative momentum regions ($q_i \leqslant 200$ MeV/c; $q_{j,k} \leqslant 30$ MeV/c) are about 2.7%$N_{\pi\pi}$, where i, j, and k denote the directions of "out", "side", and "long". In Fig. 4, the dot-dashed, dashed, and solid lines are the corresponding fitting curves.

Figures 5(a), (b), (c), and (d) show the fit results $R_{\rm o}$, $R_{\rm s}$, $R_{\rm l}$, and $R_{\rm o} - R_{\rm s}$ for different freeze-out temperatures and as a function of impact parameter. From Fig. 5(a), (b), and (c) we can see that the HBT radii decrease with impact parameter increasing. The reason is that the source size decreases when the impact parameter increases. Because the source size is larger at lower temperature, the HBT radii for lower freeze-out temperature are larger than those for higher freeze-out temperature. The difference between the HBT radii $R_{\rm o}$ and $R_{\rm s}$ includes the information about the duration of pion emission $\delta\tau$ [11, 30]:

$$R_{\rm o}^2 \approx R_{\rm s}^2 + \beta_{\rm T}^2 (\delta\tau)^2 , \quad (2)$$

where $\beta_{\rm T}$ is the average transverse velocity of the pair. For a certain impact parameter, the difference between $R_{\rm o}$ and $R_{\rm s}$ increases with the decrease of the freeze-out temperature. This is because that the average pair velocity and freeze-out time are larger for a lower $T_{\rm f}$. For a larger impact parameter, the energy density and size of the source are smaller. This leads to smaller $\beta_{\rm T}$ and $\delta\tau$, and then smaller $R_{\rm o} - R_{\rm s}$.

In Fig. 6 we exhibit the $R_{\rm o}$, $R_{\rm s}$, and $R_{\rm o}/R_{\rm s}$ as a function of $K_{\rm T} = (p_{1\rm T} + p_{2\rm T})/2$ obtained by our simulated calculations with NEXSPHERIO. We also plot the RHIC experimental data [31] for comparison. One can see that the $K_{\rm T}$ dependence either of the $R_{\rm o}$ or $R_{\rm s}$ is flatter than that of the corresponding

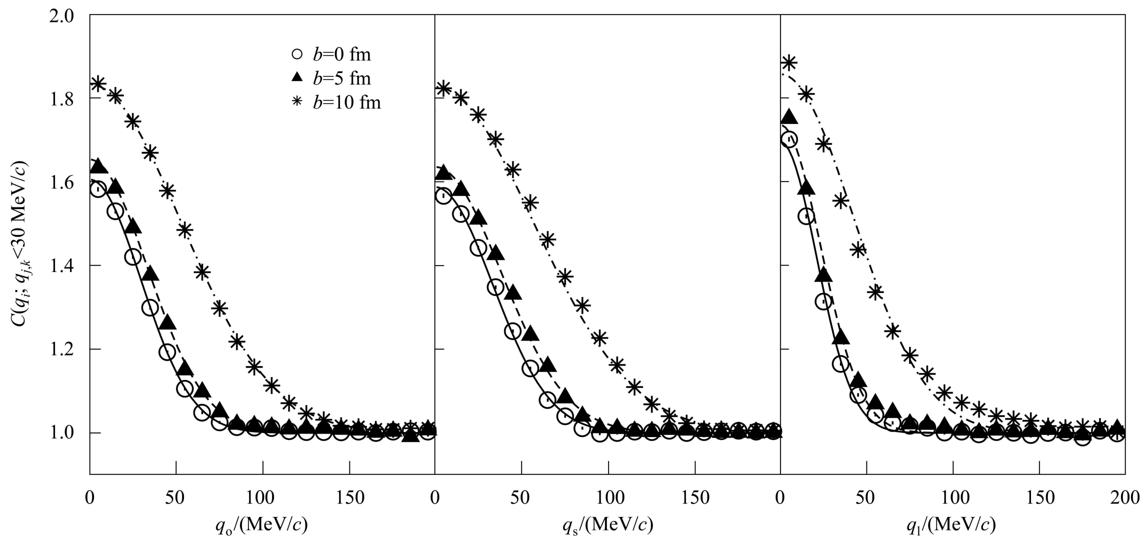

Fig. 4. Two-pion correlation functions in NEXSPHERIO model. The symbols ∘, △, and ∗ are for $b=0$ fm, $b=5$ fm and $b=10$ fm, respectively. The lines are the fitting curves.

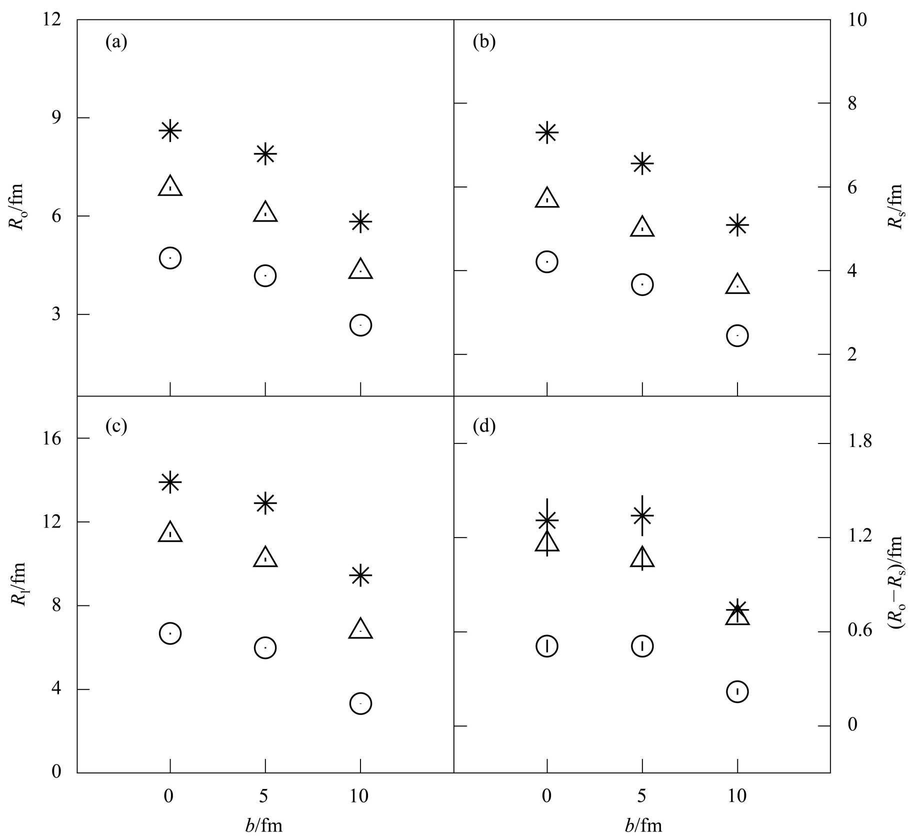

Fig. 5. The HBT radii for different freeze-out temperatures and impact parameters. The symbols ∘, △, and ∗ are for the freeze-out temperatures $T_{\rm f}=150$ MeV, $T_{\rm f}=130$ MeV and $T_{\rm f}=110$ MeV, respectively.

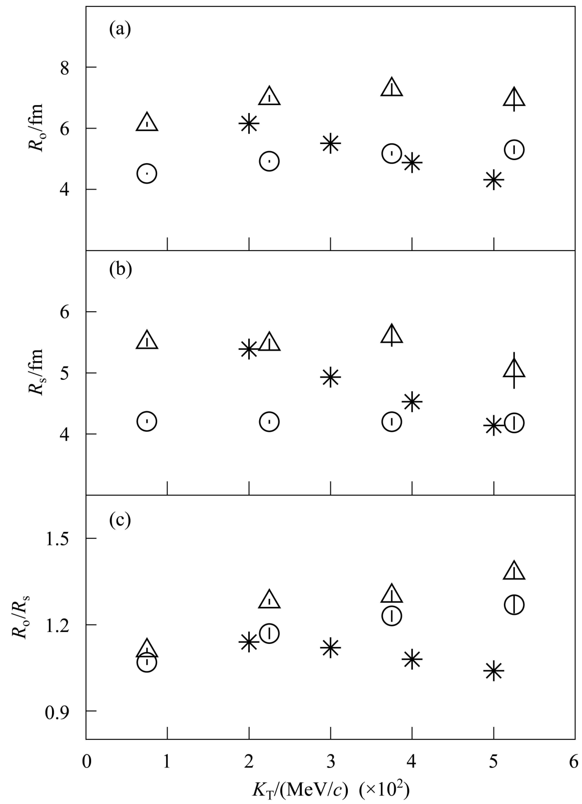

Fig. 6. Two-pion HBT radii as a function of K_T. The symbols ∘ and △ are for T_f =150 and 130 MeV. The symbols ∗ are the RHIC experimental data of STAR [31].

experimental data. It is consistent with the other hydrodynamical calculations [6, 32, 33] although the continuous emission model can lead to a more m_T dependence of R_s [6]. From Fig. 6(c) it can be seen that the values of R_o/R_s for the higher freeze-out temperature are smaller, which reflects the smaller duration of pion emission for the higher T_f condition. Our HBT results of the ratio R_o/R_s are between 1.0 and 1.4. They are consistent with the previous results in the NEXSPHERIO model [6] and smaller than those of the hydrodynamical calculations with smoothed initial conditions [32, 33]. Recently, a granular source model of QGP droplets evolving hydrodynamically [7] and a hydrodynamical model with Gaussian initial energy distribution and a very high initial central temperature [34] can reproduce the experimental transverse-momentum spectra, elliptic-flow, and HBT radii in the collisions of $\sqrt{s_{NN}} = 200$ GeV Au+Au. Comparing the HBT results as well as other observables in these models and investigating the reasons of their differences will be of interest in the future.

4 Conclusion

We examine the space-time structure of the particle-emitting source and two-pion interferometry in the NEXSPHERIO model with a crossover-transition EOS. In an event-by-event basis, the initial matter distribution in high energy heavy ion collisions is fluctuated. This kind of fluctuating initial conditions lead to inhomogeneous particle-emitting sources with granular-lump structure. The number of the lumps is larger for the event with smaller impact parameter.

By applying the interferometry analysis for simulated two-pion correlation events, we find that the HBT radii increase with the decrease of the freeze-out temperature T_f and impact parameter b. The difference between the HBT radii R_o and R_s increases with the decrease of T_f because the average pair velocity and freeze-out time are larger for a lower T_f. For a larger b, the smaller energy density and source size lead to smaller $R_o - R_s$. The K_T dependence either of the R_o or R_s in our calculations is flatter than that of the corresponding experimental data, and consistent with the other hydrodynamical calculations [6, 32, 33]. Our results of R_o/R_s are between 1.0 and 1.4. They are consistent with the previous results in the NEXSPHERIO model and smaller than those of the hydrodynamical calculations with smoothed initial conditions [32, 33]. Comparing the HBT results as well as other observables in different hydrodynamical models and investigating the reasons of their differences will be of interest in the future.

References

1 Rischke D H. nucl-th/9809044
2 Kolb F, Heinz U. nucl-th/0305084
3 Akkelin S V, Hama Y, Karpenko Iu A, Sinyukov Yu M. Phys. Rev. C, 2008, **78**: 034906
4 Hirano T, Kolk N, Bilandzic A. arXiv:0808.2684[nucl-th]
5 Gyulassy M, Rischke D H, ZHANG B. Nucl. Phys. A, 1997, **613**: 397
6 Socolowski Jr O, Grassi F, Hama Y, Kodama T. Phys. Rev. Lett., 2004, **93**: 182301
7 ZHANG W N, REN Y Y, Wong C Y. Phys. Rev. C, 2006, **74**: 024908
8 REN Y Y, ZHANG W N, LIU J L. Phys. Lett. B, 2008, **669**: 317
9 YANG Z T, ZHANG W N, HUO L, ZHANG J B. J. Phys. G, 2009, **36**: 015113
10 Wong C Y. Introduction to High-Energy Heavy-Ion Collisions. Singapore: World Scientific, 1994, Chap. 17
11 Wiedemann U A, Heinz U. Phys. Rept., 1999, **319**: 145
12 Weiner R M. Phys. Rept., 2000, **327**: 249
13 Lisa M A, Pratt S, Soltz R, Wiedemann U A. Annu. Rev. Nucl. Sci., 2005, **55**: 357; nucl-ex/0505014
14 Aguiar C E, Kodama T, Osada T, Hama Y. J. Phys. G, 2001, **27**: 75
15 Gaździcki M, Gorenstein M I, Grassi F, Hama Y, Kodama T, Socolowski Jr O. Braz. J. Phys., 2004, **34**: 322
16 Hama Y, Kodama T, Socolowski Jr O. hep-ph/0407264
17 ZHANG W N, Efaaf M J, Wong C Y. Phys. Rev. C, 2004, **70**: 024903
18 ZHANG W N, LI S X, Wong C Y, Efaaf M J. Phys. Rev. C, 2005, **71**: 064908
19 Drescher H J, LIU F M, Ostapchenko S, Pierog T, Werner K. Phy. Rev. C, 2002, **65**: 054902
20 Hama Y, Andrade R P G, Grassi F, Socolowski Jr O, Kodama T, Tavares B, Padula S S, Nucl. Phys. A, 2006, **774**: 169
21 Andrade R, Grassi F, Hama Y, Kodama T, Socolowski Jr O. Phys. Rev. Lett., 2006, **97**: 202302
22 Andrade R P G, Grassi F, Hama Y, Kodama T, Qian W L. Phys. Rev. Lett., 2008, **101**: 112301
23 Blaizot J P, Ollitrault J Y. Phys. Rev. D, 1987, **36**: 916
24 Learmann E. Nucl. Phys. A, 1996, **610**: 1
25 Rischke D H, Gyulassy M. Nucl. Phys. A, 1996, **608**: 479
26 STAR Collaboration, Adams J et al. Nucl. Phys. A, 2005, **757**: 102
27 PHENIX Collaboration, Adcox K et al. Nucl. Phys. A, 2005, **757**: 184
28 Pratt S. Phys. Rev. D, 1986, **33**: 72; Pratt S, Csörgo T, Zimányi J. Phys. Rev. C, 1990, **42**: 2646
29 Bertsch G, Gong M, Tohyama M. Phys. Rev. C, 1988, **37**: 1896; Bertsch G. Nucl. Phys. A, 1989, **498**: 173c
30 Chapman S, Scotto P, Heinz U. Phys. Rev. Lett, 1995, **74**: 4400
31 STAR Collaboration, Adams J et al. Phys. Rev. C, 2005, **71**: 044906
32 Heinz U, Kolb P. Uncl. Phys. A, 2002, **702**: 269c
33 Hirano T, Morita K, Muroya S and Nonaka C. Phys. Rev. C, 2002, **65**: 061902; Hirano T, Tsuda K. Phys. Rev. C, 2002, **66**: 054905
34 Broniowski W, Chojnacki M, Florkowski W, Kisiel A. Phys. Rev. Lett., 2008, **101**: 022301; Chojnacki M, Florkowski W, Broniowski W, Kisiel A. Phys. Rev. C, 2008, **78**: 014905